# Supporting Information for

## Seagrass-inspired Design of Soft Photocatalytic Sheets Based on Hydrogel-integrated Free-standing 2D Nanoassemblies of Multifunctional Nanohexagons

*Zijun Yong, Lim Wei Yap, Runfang Fu, Qianqian Shi, Zhirui Guo, Wenlong Cheng**

Department of Chemical Engineering, Faculty of Engineering, Monash University, Clayton, 3800, Victoria, Australia

* Correspondence to: wenlong.cheng@monash.edu

## Experimental section

***Chemicals:*** Gold (III) chloride trihydrate ($HAuCl_4 \cdot 3H_2O$, ≥99.9%), hexadecyltrimethylammonium bromide (CTAB), cetyltrimethylammonium chloride (CTAC), L-ascorbic acid (AA), silver nitrate ($AgNO_3$), palladium chloride ($PdCl_2$, 99%), hexamethylenetetramine (HMT), thioacetamide (TAA), cadmium acetate ($Cd(Ac)_2$), methylene blue (MB), methyl orange (MO), and polyvinylpyrrolidone (PVP, Mn=40,000 g/mol) were obtained from Sigma-Aldrich. Sodium hydroxide (NaOH) was purchased from Merck. Absolute ethanol (EtOH) was purchased from Ajax Finechem. Chloroform was purchased from EMSURE. UltraPure agarose was purchased from Invitrogen. Milli-Q water was obtained from Milli-Q Advantage A 10 water purification System. All materials were directly used without any further purification.

***Synthesis of Au nanohexagons (NHs):*** The detailed procedure can be referred to our previous work.[1]

***Synthesis of Au-Pd NHs:*** Au-Pd NHs was synthesized through under-potential deposition method with a slightly modification.[2] 30 ml of the above Au NHs was mixed with 30 ml of 0.1 M CTAB in the 30 $^oC$ water bath with stirring. Then, 2 ml of 0.1 M AA, 120 ul of 10 mM $AgNO_3$, and 3 ml of 0.1 M NaOH were added the previously prepared Au NHs suspension and vigorously stirred for 30 min. The resulting Au@Ag core-shell NHs was collected by centrifugation with 3200 rpm for 9 min, and then redispersed into 60 ml of Milli-Q water. Next, 0.5 ml of 2 mM AA and 1 ml 2 mM $H_2PdCl_4$ were added into the above Au@Ag NHs solution and stirred in the 30 $^oC$ water bath for 2 min. Then, the mixture was kept undisturbed for 1 hr

and centrifuged with 3200 rpm for 10 min to achieve Au-Pd NHs, and then redispersed into 30 ml of Milli-Q water for further use.

***Synthesis of Au-Pd-CdS mNHs:*** Au-Pd-CdS mNHs was fabricated by deposition CdS layer on the Au-Pd NHs through chemical bath deposition.[3] 6 ml of 0.1 M CTAC, 6 ml of 0.1 M AA, and 6 ml of 0.1 M HMT were added into the above Au-Pd NHs aqueous solution and stirred in the 80 $^{o}$C water bath for 1 min. After that, 120 ul of 0.1 M TAA and 90 ul of 10 mM $Cd(Ac)_2$ were added and stirred for 1 hr. The final product was centrifuged with 3200 rpm for 10 min, and then redispersed into 30 ml of Milli-Q water for further use.

***Synthesis of Au-CdS NHs:*** The preparation of Au-CdS NHs was same as the synthetic process of Au-Pd-CdS mNHs, only replacing Au-Pd NHs with Au NHs.

***Synthesis of CdS nanoparticles:*** The preparation of CdS nanoparticles was same as the synthetic process of Au-CdS NHs with no addition of Au NHs.

***Fabrication of 2D Au-Pd-CdS mNHs assemblies:*** The Au-Pd-CdS mNHs assemblies were fabricated by our recently developed approach with a slightly modification.[4] Firstly, CTAB/CTAC surfactants were replaced by PVP (Mn = 40,000 g/mol) by dispersing 24 ml of CTAB/CTAC-capped nanoparticles into 12 ml of 4 mg/ml PVP/EtOH solution. After the overnight ligand exchange, the PVP-capped Au-Pd-CdS mNHs was washed two times with EtOH, and finally redispersed into chloroform. After that, the concentrated solution was achieved by removing the supernatant, and then dropped upon the surface of a sessile water

droplet on Si wafer or ITO glass. As the water droplet evaporated, Au-Pd-CdS mNHs assemblies were obtained. Au NHs, Au-Pd NHs, and Au-CdS NHs assemblies were also prepared under the same condition.

***Fabrication of hydrogel-integrated 2D Au-Pd-CdS mNHs assemblies:*** Similar as the above procedure to prepare nanoassemblies on Si wafer, the concentrated Au-Pd-CdS mNHs in chloroform was dropped onto a pancake-like water film sitting on aluminium foil. After drying, the nanoassemblies was treated by air plasma for 2 mins and 1 ml of heated 1% agarose solution was drop-casted on the nanoassemblies. After cooling and gelation, hydrogel was successfully formed on the top of nanoassemblies. Then, aluminium foil was easily removed from nanoassemblies by immerging into 10 ml of 0.1 M NaOH solution for about 10 mins. The whole etching process was conducted at room temperature (~20 $^{o}$C) with a pH of 13.51 for a short reaction time (~10 mins). This led to the formation of the hydrogel-integrated 2D nanoassemblies which didn't appear to be affected by the etching process.

***Fabrication of soft artificial seagrass:*** Due to the soft hydrogel, the hydrogel-integrated Au-Pd-CdS mNHs assemblies was cut into several small ribbons and inserted into a mould made of 5 ml of heated 1% agarose solution. After curing, soft artificial seagrass was successfully fabricated.

***Photocatalytic Activity Measurement:*** The photocatalytic performances of nanoparticles suspension, 2D nanoassemblies, and random-packing film were measured by the photodegradation of MB under simulated sunlight irradiation (xenon lamp, 300W) at room

temperature. For the catalysts dispersing in the solution, 5 ml of nanoparticles suspension was centrifugated to remove excess supernatants, followed by the addition of 2 ml of 5 μg/ml MB aqueous solution. To get the kinetic reaction curve, UV-Vis absorption spectra (Agilent 8453 UV-Vis Spectrophotometer) of reaction solution were recorded for a regular interval time of 10 min. For nanoassemblies, each sample with an area of ~0.2 $cm^2$ on silicon wafer was dipped into 2 ml of 5 μg/ml MB aqueous solution to examine their photocatalytic performance. For the nanoassemblies on ITO glass and hydrogel, the photodegradation rates were obtained under the same condition of nanoassemblies on Si wafer. Random-packing film was prepared by drop-casting 2 ml of Au-Pd-CdS mNHs solution to get a film with an area of 1*1 $cm^2$. Its photocatalytic performance was measured by immersing randon-packing film into 2 ml of 5 μg/ml MB aqueous solution. All the photodegradation rates were compared by normalizing Au amount. For soft artificial seagrass, 18 ml of 5 μg/ml MB aqueous solution was used for photodegradation. For the light intensity-dependent photocatalytic reaction, the light intensity was measured by power meter (Newport, 843-R). For the photodegradation of MO, each nanoassemblies with an area of ~0.2 $cm^2$ on silicon wafer was dipped into 2 ml of 5 μg/ml MO aqueous solution to examine their photocatalytic performance.

***Characterization:*** The morphologies colloidal nanoparticles and their corresponding nanoassemblies were measured through scanning electronic microscope (SEM) (FEI Magellan 400 FEGSEM operating at 5 kV) and transmittance electronic microscope (TEM) (FEI Tecnai G2 T20 TWIN LaB6 TEM operating at 200 kV). The voidage was estimated using ImageJ image analysis software. In particular, the SEM image was imported into the software and converted into a binary image. The threshold of the new image was adjusted manually to include all the particles and then the area of the voidage was analysed using the automated analyze function in the software. The elements distribution of Au, Pd, Cd, and S were analysed

by scanning TEM (STEM) coupled with energy dispersive X-ray spectroscopy (EDS) (FEI Tecnai G2 F20). Agilent 8453 UV-Vis Spectrophotometer was used to record the extinction spectra of all nanoparticle suspensions and nanoassemblies on ITO glass and hydrogel. X-ray diffraction (XRD) patterns were recorded on a Rigaku Miniflex600 powder diffractometer with Cu Kα radiation (λ=1.54056 Å) from 10º to 90º. Concentrations of Au ion of photocatalysts including nanoparticles dispersing in the solution, random packing film, and 2D nanoassemblies were quantified by an inductively coupled plasma emission spectroscopy (ICP-OES, Perkin Elmer Optima 7000 DV ICP-OES) by dissolving samples into aqua regia. The Au amount of each sample for photocurrent test was also achieved by ICP test. Photoelectrochemical (PEC) tests for the random-packing films and their corresponding nanoassemblies were operated on an electrochemical workstation (CHI 660E, Chenhua, US) in a three-electrode system with 0.5 M $Na_2SO_4$ aqueous solution as electrolyte under simulated sunlight irradiation with 1 sun intensity. Platinum foil and Ag/AgCl electrode were used as counter and reference electrodes, respectively. Working electrodes for random-packing films were formed by drop-casting the concentrated nanoparticles solution on fluorine-doped tin oxide (FTO) glasses, and for nanoassemblies, PVP-capped nanoparticles were assembled on the surface of a pancake-like water film on FTO glasses, and then dried at room temperature. Note that the volumes of nanoparticles using for drop-casting random-packing films and preparing nanoassemblies kept constant, and the area of each sample was set as 1 $cm^2$. Transient photocurrent responses were recorded at an external 0.4 V bias.

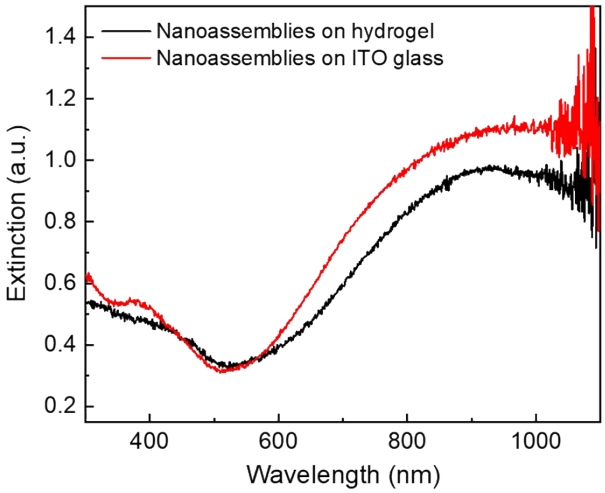


**Figure S1**. Extinction spectrum of Au-Pd-CdS mNHs assemblies supported by different substrates: hydrogel (black line) and ITO glass (red line).

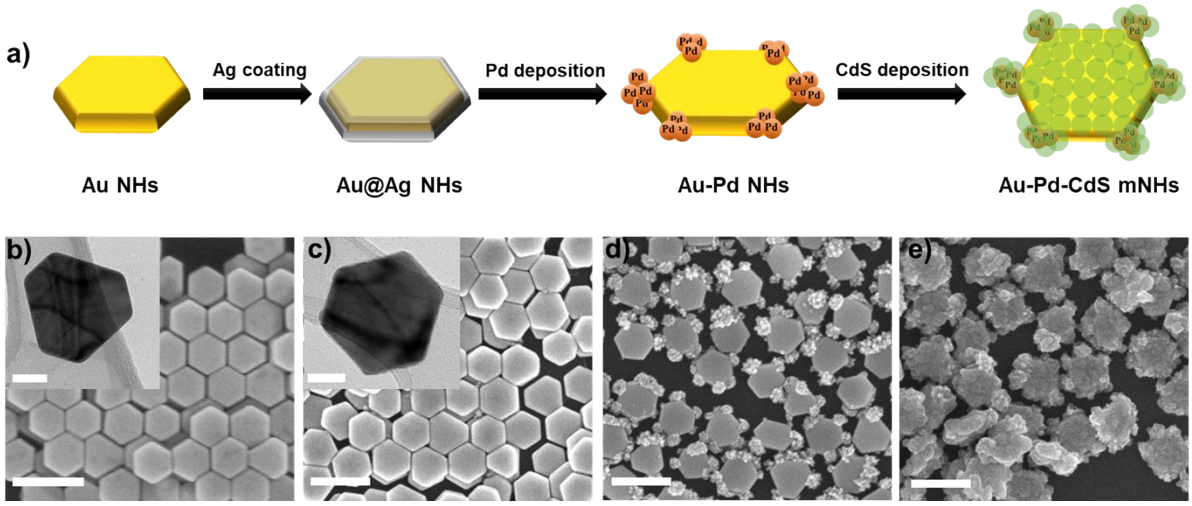


**Figure S2**. a) Schematic illustration of the fabrication of Au-Pd-CdS hybrid nanoparticles. b-e) SEM images of b) Au NHs; c) Au@Ag NHs; d) Au-Pd NHs; and e) Au-Pd-CdS mNHs discrete nanoparticles. Inserts in b) and c) are their corresponding TEM images. The scale bar for SEM is 200 nm, for TEM is 50 nm.

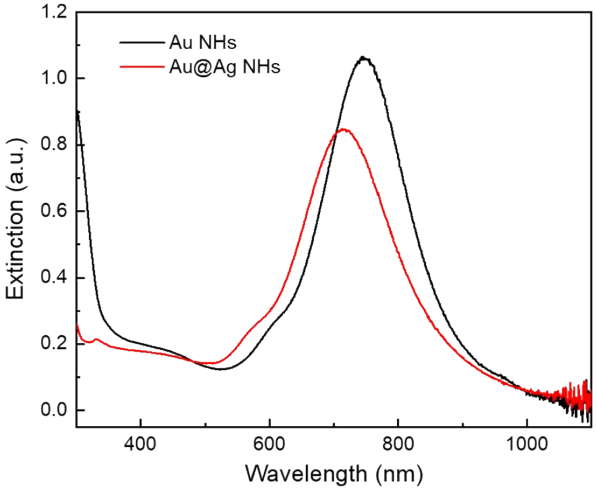


**Figure S3**. Extinction spectra of Au NHs (black line) and Au@Ag NHs (red line) dispersing in the aqueous solution.

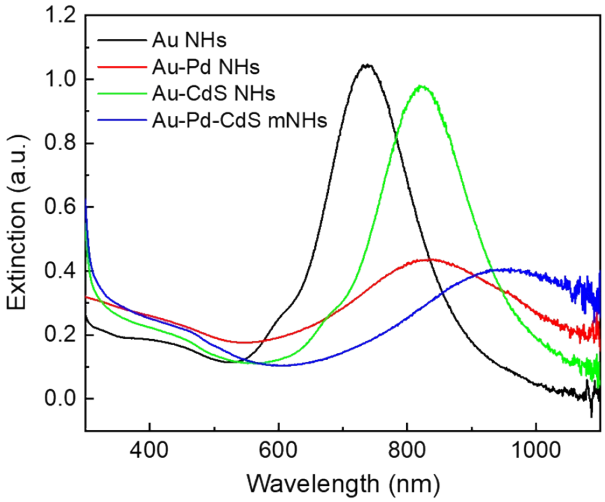


**Figure S4**. Extinction spectra of Au NHs (black line), Au-Pd NHs (red line), Au-CdS NHs (green line), and Au-Pd-CdS mNHs (blue line) dispersing in the aqueous solution.

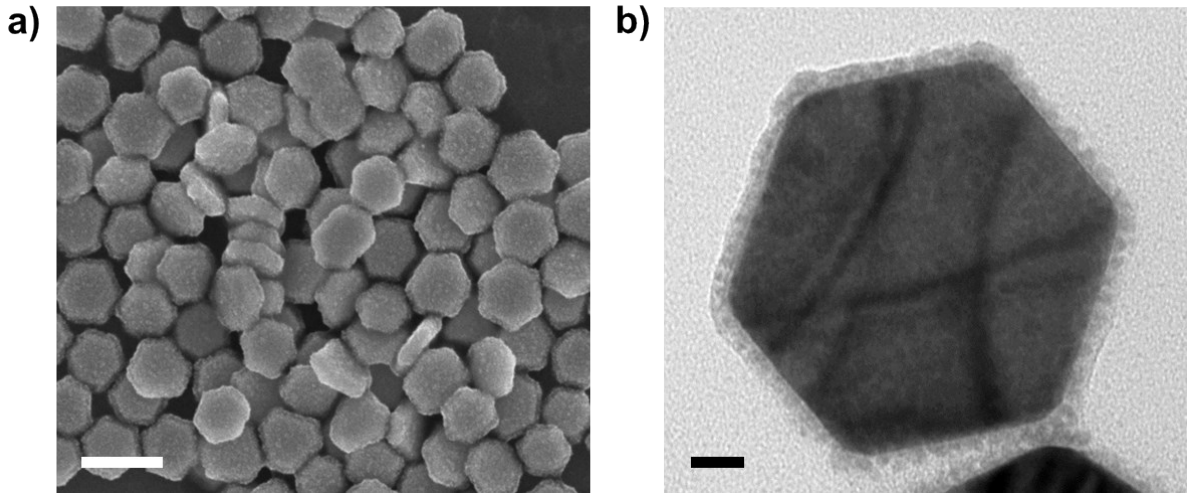


**Figure S5**. a) SEM and b) TEM image of Au-CdS NHs. Scale bar is 200 nm for SEM image, 20 nm for TEM image.

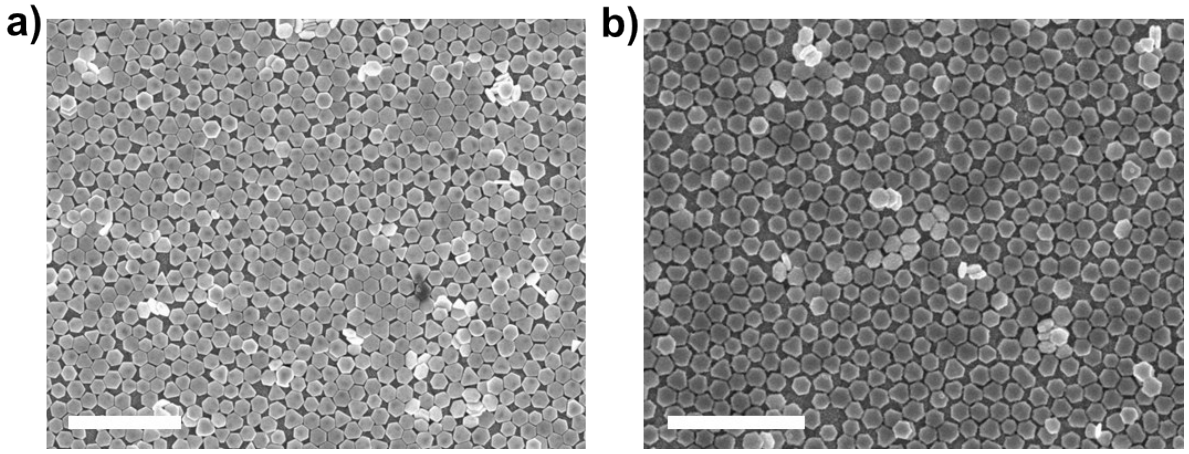


**Figure S6**. SEM images of a) Au NHs and b) Au-CdS NHs assemblies. Scale bar is 1 μm.

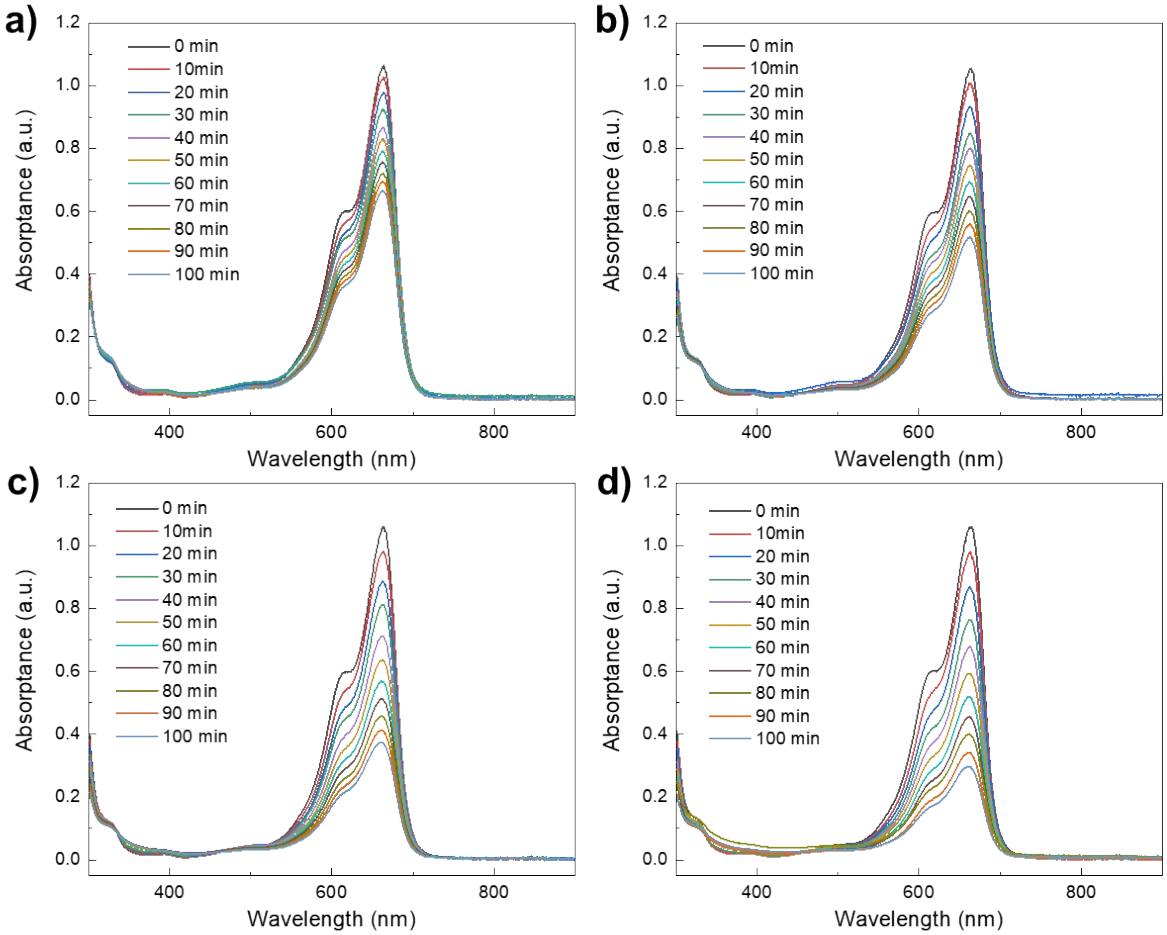


**Figure S7.** UV-Vis absorption spectra of MB solution with nanoassemblies during the photodegradation process under light irradiation: a) Au NHs; b) Au-Pd NHs; c) Au-CdS NHs; d) Au-Pd-CdS mNHs.

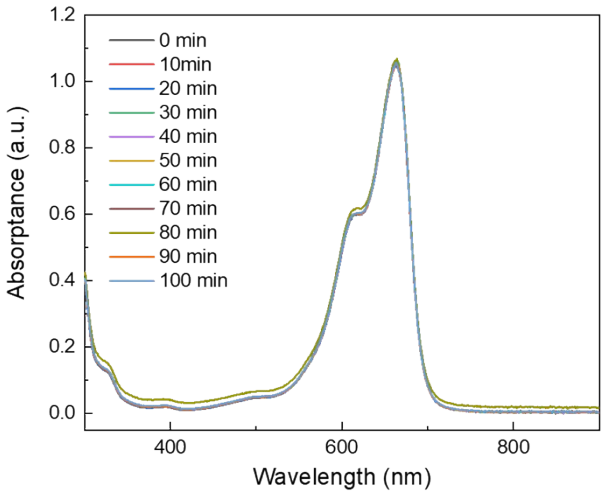


**Figure S8.** UV-Vis absorption spectra of MB solution with Au-Pd-CdS mNHs assemblies in dark.

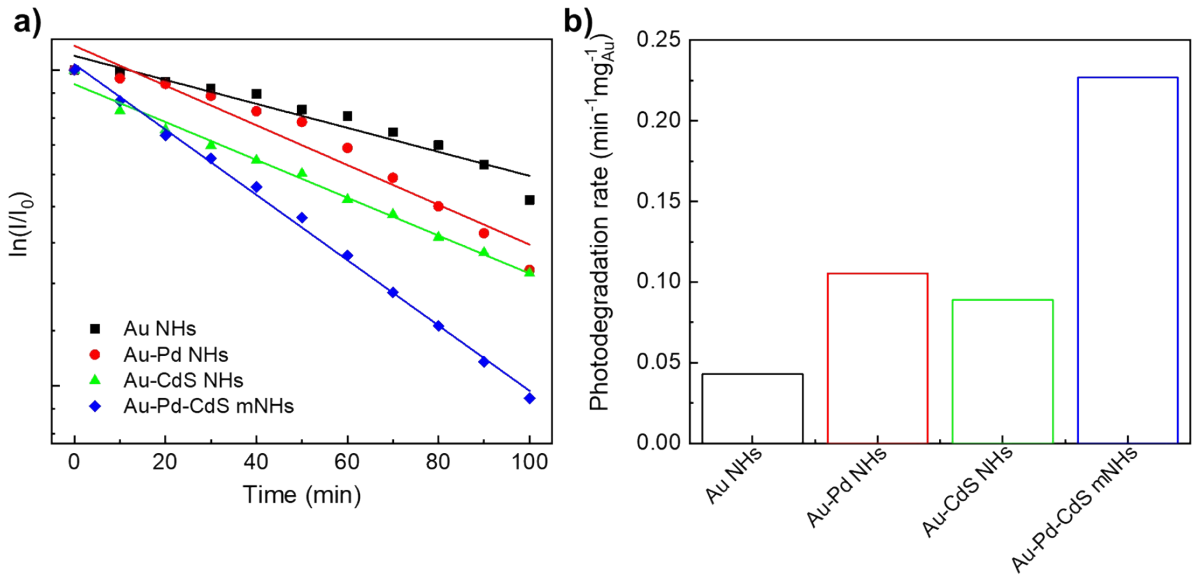


**Figure S9.** a) Plots of $\ln(I/I_0)$ versus reaction time after different colloidal nanoparticles in the MB solution under light irradiation; b) Photodegradation rates of MB for different discrete nanoparticle suspensions by normalizing Au amount. Au amount of each sample was measured by ICP test (**Table S1**).

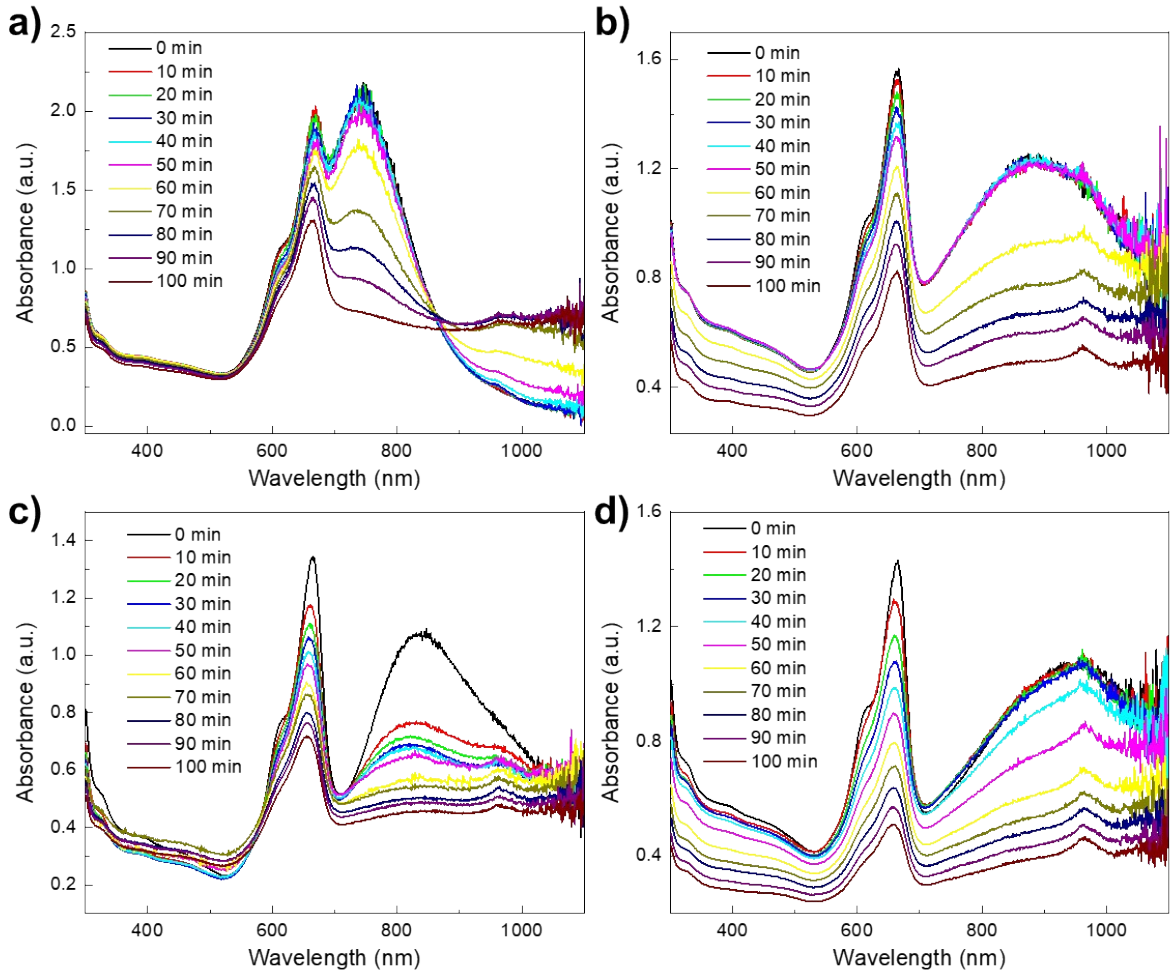


**Figure S10.** UV-Vis absorption spectra of MB solution by adding nanoparticle solution under light irradiation: a) Au NHs; b) Au-Pd NHs; c) Au-CdS NHs; d) Au-Pd-CdS mNHs.

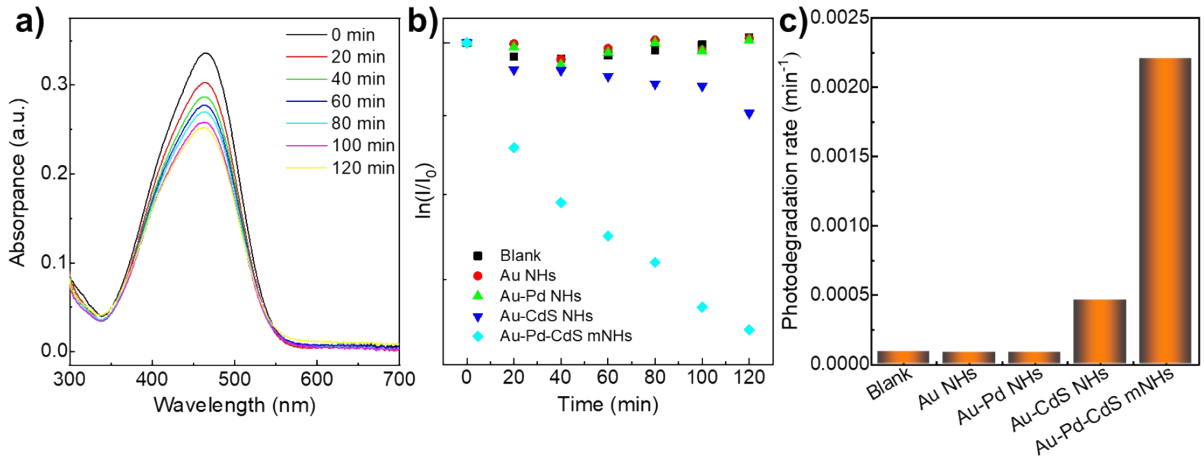


**Figure S11.** a) UV-Vis absorption spectra of methyl orange (MO) solution (5 μg/ml) by adding Au-Pd-CdS mNHs assemblies under light irradiation; b) Plots of $\ln(I/I_0)$ versus reaction time over different nanoassemblies on Si wafer with an area of ~0.2 $cm^2$ in the photodegradation of MO; c) Corresponding photodegradation rates of MO for different nanoassemblies.

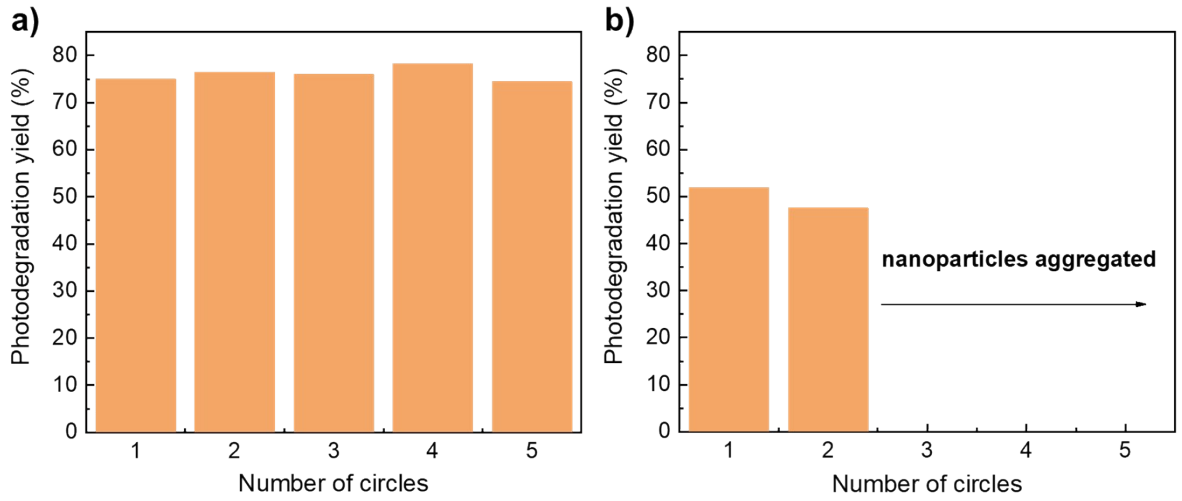


**Figure S12.** Photodegradation yield of MB over a) Au-Pd-CdS mNHs assemblies on Si wafer and b) its corresponding nanoparticles dispersing in the solution under light irradiation for 2 hours in 5 consecutive reaction cycles without a regeneration of photocatalysts. After each cycle, nanoassemblies was washed with MQ-water, dried with $N_2$, and immersed into new MB solution to start a new cycle. For nanoparticles suspension, the final solution was centrifuged and redispersed into a new MB solution for the next cycle.

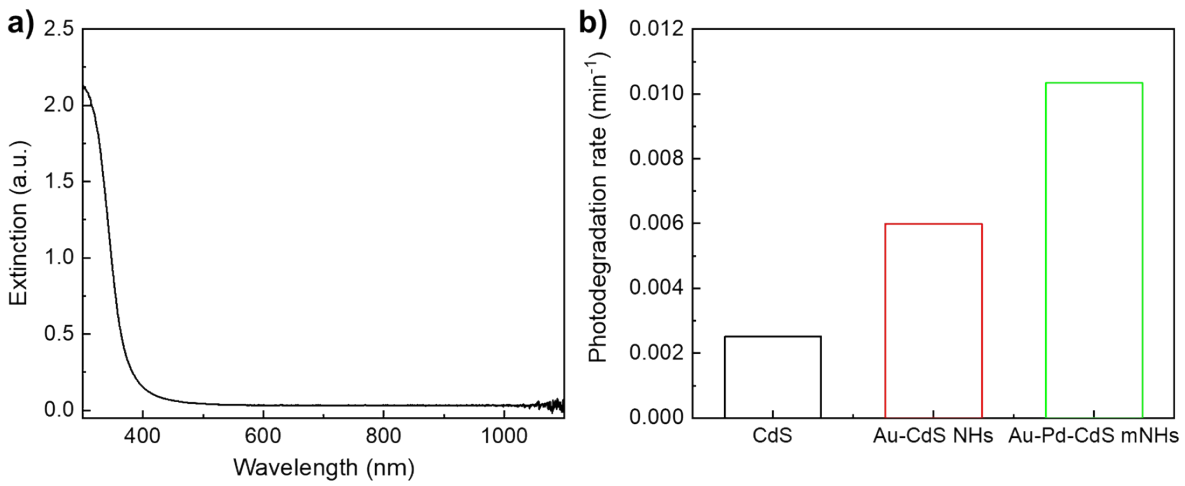


**Figure S13.** a) UV-Vis spectrum of CdS aqueous solution. b) MB photodegradation rates of CdS, Au-CdS NHs, and Au-Pd-CdS mNHs dispersing in the solution.

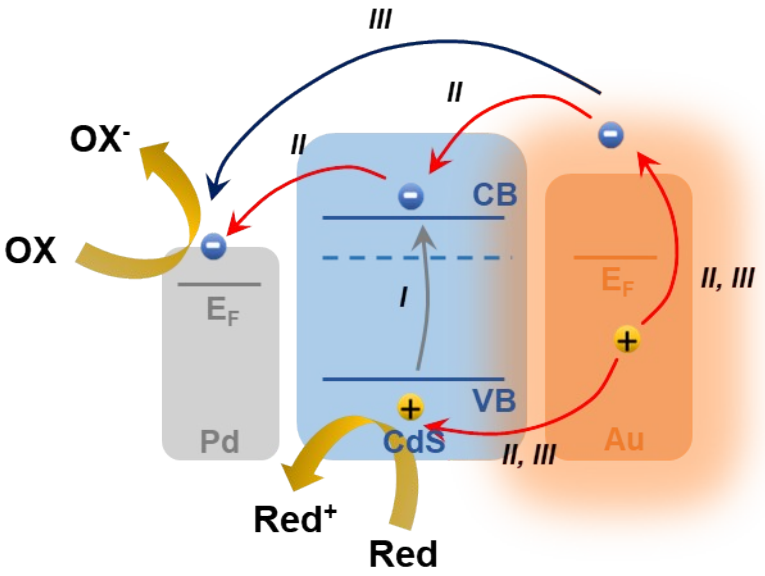


**Figure S14**. Mechanism illustration of electron transfer pathways in the Au-Pd-CdS mNH.

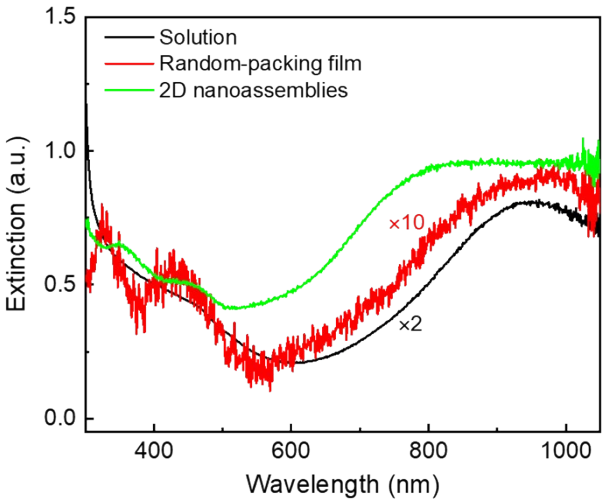


**Figure S15**. Extinction spectra of Au-Pd-CdS mNH soluiton (black line), random-packing film (red line), and 2D nanoassemblies (green line).

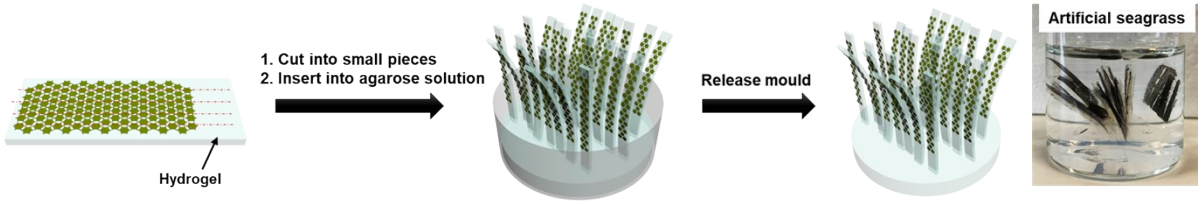


**Figure S16.** Schematic illustration of the fabrication process of soft artificial seagrass.

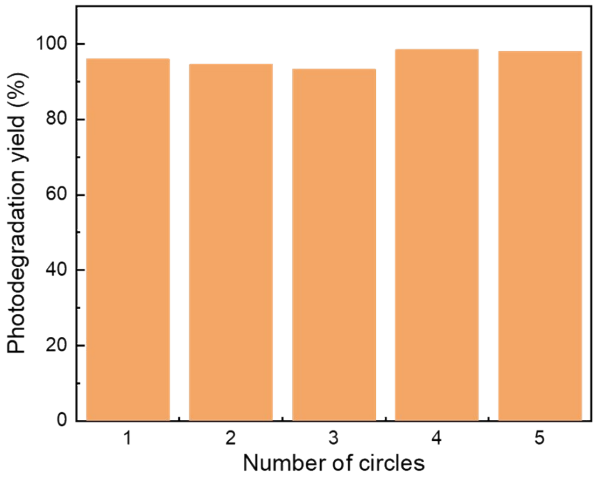


**Figure S17**. MB photodegradation yield of soft artificial seagrass within 150 min reaction in 5 consecutive reaction cycles without the need of catalyst regeneration. After each cycle, the reacted solution was removed and 18 ml of new MB solution was added to start a new cycle.

**Table S1.** ICP results and the corresponding Au amounts using in the different photocatalysts. The ICP samples were prepared by dissolving photocatalysts into 0.5 ml aqua regia followed by adding 4.5 ml MQ-water.

| **Photocatalysts** | | **Au/ppm** | **Au amount/mg** |
|---|---|---|---|
| Nanoparticles suspension | Au NHs | 17.66 | 0.0883 |
| | Au-Pd NHs | 11.95 | 0.0598 |
| | Au-CdS NHs | 13.47 | 0.0674 |
| | Au-Pd-CdS NHs | 9.12 | 0.0456 |
| 2D nanoassemblies | Au NHs | 3.25 | 0.0163 |
| | Au-Pd NHs | 1.89 | 0.0095 |
| | Au-CdS NHs | 1.87 | 0.0094 |
| | Au-Pd-CdS NHs | 0.81 | 0.0041 |
| Random-packing film | Au-Pd-CdS NHs | 1.05 | 0.0052 |

**Table S2.** ICP results and the corresponding Au amounts of samples for photocurrent test. The ICP samples were prepared by dissolving samples on FTO glass into 0.5 ml aqua regia followed by adding 4.5 ml MQ-water.

| **Photocurrent samples** | | **Au/ppm** | **Au amount/mg** |
|---|---|---|---|
| 2D nanoassemblies | Au NHs | 6.08 | 0.0304 |
| | Au-Pd NHs | 6.04 | 0.0302 |
| | Au-CdS NHs | 7.78 | 0.0389 |
| | Au-Pd-CdS NHs | 4.85 | 0.0243 |
| Random-packing film | Au NHs | 3.55 | 0.0177 |
| | Au-Pd NHs | 2.95 | 0.0147 |
| | Au-CdS NHs | 3.08 | 0.0154 |
| | Au-Pd-CdS NHs | 2.40 | 0.0120 |

## References


1. Z. Yong, Q. Shi, R. Fu, W. Cheng, *Adv. Mater. Interfaces,* 2021, **8**, 2001686.

2. C. Shan, E. T. Martin, D. G. Peters, J. M. Zaleski, *Chem. Mater.,* 2017, **29**, 6030-6043.

3. L. Ma, K. Chen, F. Nan, J. H. Wang, D. J. Yang, L. Zhou, Q. Q. Wang, *Adv. Funct. Mater.,* 2016, **26**, 6076-6083.

4. D. Dong, R. Fu, Q. Shi, W. Cheng, *Nat. Protoc.,* 2019, **14**, 2691-2706.